

Effect of co-gasification of biomass and petroleum coke with coal on the production of gases

J. Feroso<sup>a</sup>, B. Arias<sup>a</sup>, B. Moghtaderi<sup>b</sup>, C. Pevida<sup>a</sup>, M.G. Plaza<sup>a</sup>, J.J. Pis<sup>a</sup>, F. Rubiera<sup>a\*</sup>

<sup>a</sup> Instituto Nacional del Carbón, INCAR-CSIC. Apartado 73, 33080 Oviedo, Spain

<sup>b</sup> Priority Research Centre for Energy, School of Engineering, Faculty of Engineering and Built Environment, The University of Newcastle, University Drive, Callaghan, NSW 2308, Australia.

## Abstract

The co-pyrolysis and co-gasification of binary blends of a bituminous coal (PT), a petcoke (PC) and two types of biomass (olive stones, OS; chestnut, CH) were studied at atmospheric pressure in a fixed bed reactor. The pyrolysis and gasification were performed under nitrogen, and steam/oxygen atmospheres, respectively. In a fixed bed reactor, the particles of the different fuels are in close contact, providing an optimum means for evaluating possible synergetic effects. Pyrolysis tests showed a lack of chemical interaction between the components of the blend. Therefore, the composition of the gas produced during the pyrolysis tests can be predicted from those of the individual components and their mass fractions. During the co-gasification tests, different interactions were observed depending on the heating rate. Low heating rates produced higher amount of CO and CO<sub>2</sub>, whereas tar yield decreased. At high heating rates, the biomass and coal blends produced more tar but less H<sub>2</sub> and CO. The effect of co-gasification on apparent thermal efficiency was also evaluated.

*Keywords:* co-gasification, biomass, hydrogen, coal.

## Introduction

The energy systems of most of the developed countries are based on the use of fossil fuels, and the energy demand is continuously increasing. The limited reserves are leading to a heavy dependence on imported fuels. Additionally, the use of fossil fuels leads to production of pollutants and have a very negative impact on the environment, especially from the point of view of CO<sub>2</sub> emissions and the implications for global warming. For these reasons, one of the current challenges of energy production is to reduce the dependence on fossil fuels and to

---

\* Corresponding author. Tel.: +34 985 118 975; Fax: +34 985 297 662.

E-mail address: frubiera@incarcsic.es (F. Rubiera)

create a more sustainable scenario. One of the most promising approaches for diversifying energy resources is that of renewable energy, due to its less harmful environmental impact than fossil fuels, and its potential contribution to preserving the equilibrium of ecosystems. Moreover, renewable energies are indigenous resources, and an increase in their use will have positive implications for the security of supplies. Among the different renewable energy resources available, biomass is the most promising resource for the immediate future as it is considered a carbon neutral fuel (that is the carbon dioxide released during biomass utilisation is an integral part of the carbon cycle).

On the other hand, hydrogen is generally considered to be the most promising energy carrier of the future. The use of hydrogen could reduce current dependence on fossil fuels, and contribute to reducing the negative effects of greenhouse gas emissions.<sup>1-3</sup> A hydrogen economy based on renewable energy is envisaged as essential in the long term. Nowadays, 98% of hydrogen production comes from fossil fuels and, more specifically, 50% from the reforming of natural gas.<sup>4</sup> However, drawbacks of this fuel are the instability of its price and its limited reserves. This explains the continued search for lower and more stable energy sources. The gasification of low-cost fuels could be an interesting alternative, as the fuel gas produced could be used for both energy and chemical production.<sup>5</sup> Various solid fuels, including coal, biomass, and even wastes such as petroleum coke, heavy refinery residuals and municipal sewage sludge have all been employed as feedstocks in gasification.<sup>6-10</sup> Biomass gasification has been successfully demonstrated on a large scale and a variety of biomass sources can be exploited in the gasification process.<sup>11,12</sup> However, current experience is still limited and more research is needed in order to increase the knowledge and establish a sounder basis for further progress. The co-gasification of coal and biomass can be used during the transition from fossil fuels to renewable sources.

Nevertheless, in order to obtain a clean fuel such as hydrogen by means of gasification, the CO<sub>2</sub> produced in the process must be captured and stored. Co-gasification of coal and biomass presents the advantage of a net reduction in CO<sub>2</sub> emissions, if CO<sub>2</sub> capture is contemplated in the process.

In this work, the co-pyrolysis and co-gasification of mixtures of a bituminous coal, a petcoke and two types of biomass were carried out. Pyrolysis tests were performed using nitrogen as inert gas, while mixtures of steam, nitrogen and oxygen were used for gasification tests. During the tests, the mass yield distribution in char, gas and liquids, were calculated and the gas composition was measured. The objective of this work is to study the possible synergistic

effects of using coal and biomass during pyrolysis and gasification, with a special view to producing hydrogen.

## **Experimental**

In this work, a bituminous coal (PT), a petcoke (PC), and two types of biomass, olive stones (OS) and chestnut tree residues (CH), were used. The samples were ground and sieved to obtain a fraction with a particle size of 1-2 mm. The proximate and ultimate analyses, and the high heating value of the samples used are presented in Table 1.

A quartz fixed bed reactor (20 mm internal diameter, 455 mm height) was used for the pyrolysis and gasification tests. A sample mass of around 4 g was employed in all the tests. A thermocouple in contact with the sample bed was used to measure the reaction temperature. The pyrolysis tests were carried out at a heating rate of  $15\text{ }^{\circ}\text{C min}^{-1}$  under nitrogen ( $150\text{ cm}^3\text{ min}^{-1}$ ). The gasification tests were performed using two different heating rates (15 and  $100\text{ }^{\circ}\text{C min}^{-1}$ ) under steam (70 vol. %) and oxygen (5 vol. %), carried by an inert flow of  $\text{N}_2$ , at a total flow rate of  $150\text{ cm}^3\text{ min}^{-1}$ .

During pyrolysis and gasification tests the samples were heated from room temperature up to  $1000^{\circ}\text{C}$  at a constant rate and this temperature was maintained until the end of the gas production. The liquid fraction (e.g. tars and water, etc) was separated by condensation using an ice bath. The non-condensable gases were collected in Tedlar® sample bags with a polypropylene fitting for sampling.  $\text{H}_2$ ,  $\text{N}_2$ ,  $\text{CO}$ ,  $\text{CO}_2$ ,  $\text{CH}_4$ ,  $\text{C}_2\text{H}_4$  and  $\text{C}_2\text{H}_6$  were analysed in a gas chromatograph Perkin-Elmer Sigma 15 with a TCD detector. A Teknokroma 10FT Porapak N, 60/80 and a Teknokroma 3FT Molecular Sieve 13X, 80/100 columns, were used. The system was calibrated with a standard gas mixture at periodic intervals. At the end of each test the solid fraction was weighed and the amount of gas generated during the experiment was calculated from a nitrogen balance, since the nitrogen fed and its composition in the gases evolved are known. The liquid fraction generated during the pyrolysis tests was calculated by subtracting the mass of char and produced gases from that of the initial sample.

## **Results and discussion**

### ***Pyrolysis tests***

The gas composition was determined by GC analysis, and plots of gas evolution versus time were obtained. The amount of each gas species produced during pyrolysis was calculated by integrating the area under the gas evolution plots. Table 2 shows the amounts of the main

gases produced from each fuel during pyrolysis tests. In every test (pyrolysis and gasification),  $C_2H_6$  and  $C_2H_4$  concentration remained below 0.1% and so these components are not included in the plots and tables. As can be seen from Table 2, hydrogen is the main gas produced during the pyrolysis tests. PC produces more  $H_2$  and  $CH_4$  than PT, CH and OS, despite its lowest hydrogen content. This behaviour could be attributed to the small oxygen content of PC, which prevents  $H_2O$  forming during pyrolysis. On the other hand, CH and OS produce more CO and  $CO_2$  than PC and PT, due to the high oxygen content of biomass which leads to the production of oxygenated species.<sup>13</sup>

Table 2 summarises the carbon mass distribution in gas, liquids and char during the pyrolysis tests of the individual fuels. The char yield of PC and PT were 89.1 and 61.7 %, respectively. As expected, biomass species, CH and OS, produced lower char yields during pyrolysis than fossil fuels due to the weaker strength of the macromolecular structure of these types of materials<sup>14</sup>, which results in high tar production during the pyrolysis of biomass.

Figure 1 shows  $H_2$ , CO and  $CO_2$  production during the co-pyrolysis tests. As can be seen, as the percentage of biomass increases in the blend there is a clear reduction in  $H_2$  production, whereas the level of CO and  $CO_2$  increases. On the other hand, when the percentage of PC in the PT-PC blends increases, there is an increase in  $H_2$  production and a reduction in CO and  $CO_2$ . From the results in Figure 1, it can be seen that the production of the main gaseous species during the co-pyrolysis tests follows the additive rule, there being no evidence of any chemical interaction between the components of the blends that might modify the evolution of the gas.

Figure 2 shows the mass fraction distributions in char and liquids during the pyrolysis of the PT-CH, PT-OS and PT-PC blends. For blends of PT with biomass, there is a clear reduction in char yield as the proportion of biomass in the blend increases, due to the low amount of char produced during the pyrolysis of the biomass. In contrast, there is an increase in char yield as the percentage of PC increases in the PT-PC blends.

As can be seen from Figure 2, the co-pyrolysis of coal PT and biomass followed the linear additive rule, indicating that there is no interaction between the components. Similar results have been obtained by other authors using different experimental devices, such as thermogravimetric analysers, fluidised beds, drop tube reactors and horizontal tubular reactors<sup>15-18</sup> despite the one used in this work ensures an intimate contact between particles. During the co-pyrolysis of the PT-PC blends, a similar behaviour was observed, and liquids and char production followed also the additive rule.

### *Gasification tests*

Gas production during the gasification tests of individual fuels at the two different heating rates studied are given in Table 3. CH<sub>4</sub> production during gasification tests was similar to that obtained during the pyrolysis tests, showing that the methanation reaction does not take place to any large extent and that this chemical compound is produced mainly during the pyrolysis step of the fuels.

During the gasification of coal PT at 15 °C min<sup>-1</sup>, CO<sub>2</sub> production is higher than that of CO. However, at 100 °C min<sup>-1</sup>, the opposite trend is observed and the production of CO increases. This result is accompanied by a higher H<sub>2</sub> production, indicating that at 100 °C min<sup>-1</sup>, gasification takes place to a larger extent. As the temperature increases, the reactivity of carbon towards steam also increases. If the sample is heated up at low heating rates, it has more time to react with oxygen over a range of temperatures in which carbon reactivity in steam is much lower than in oxygen. On the other hand, at higher heating rates (100 °C min<sup>-1</sup>) more of the unreacted carbon sample is able to reach high temperatures, and so its reactivity in steam is greater. Moreover, reaction of the sample at high temperatures leads to an increase in the products of the Boudouard reaction, resulting in the production of more CO.

A similar trend was observed during the gasification of the biomass samples, CH and OS. However, in these cases the reduction in CO<sub>2</sub> production at 100 °C min<sup>-1</sup> is more pronounced than at 15 °C min<sup>-1</sup>, indicating that combustion takes place to a lower extent. The petcoke, PC, shows a different behaviour since both CO and CO<sub>2</sub> production increase slightly as the heating rate rises, producing more CO<sub>2</sub> at both heating rates. This could be due to the lower reactivity of PC.

During the gasification tests, the amount of tar can not be calculated by difference as part of the gas produced proceeds from the O<sub>2</sub> and H<sub>2</sub>O that are introduced as reactants. However, it is possible to evaluate the amount of carbon that is not converted to gas and is converted to tars, as the initial carbon is known and the carbon in the gases can be calculated. Table 3 shows the amount of carbon in the tars during the gasification of the individual fuels at 15 and 100 °C min<sup>-1</sup>. During the gasification of PT and PC, there is a reduction in the amount of carbon loss in the tars with the increase in the heating rate. In contrast, there is an increase in carbon loss in the case of the biomass samples.

It is well known that the rate of mass loss during pyrolysis increases with the heating rate. This means that at 15 °C min<sup>-1</sup>, the volatile matter is released slower than at 100 °C min<sup>-1</sup>, and consequently in a longer period of time. However, during the gasification tests at both heating rates, a constant flow of oxygen is introduced into the system. For these reasons, at

15 °C min<sup>-1</sup>, the volatile matter released would have more oxygen available than at 100 °C min<sup>-1</sup>, favouring the combustion of the sample and generating more CO<sub>2</sub> (see Table 3). On the other hand, at 100 °C min<sup>-1</sup>, the ratio between oxygen and volatile matter will be smaller, and the oxidation would take place in a lower extent, producing a higher amount of tars at the exit of the reactor, and an increase in loss of carbon in tars (see Table 3). This means that the oxygen availability during the gasification tests performed in this work is influenced by the heating rate.

In the gasification of PT a different behaviour was observed. Tar production decreased as the heating rate increased. Coal PT releases a smaller amount of volatiles than biomass during gasification, and so the availability of oxygen is less restricted. In addition, coal PT devolatilises at higher temperatures than biomass and, under these conditions, its reactivity in oxygen can be expected to be higher, allowing tars to be oxidised faster. Furthermore, at these higher temperatures, the tars may be partially gasified so that less amount is produced. PC presents a similar behaviour to that of PT, and the production of tars is reduced at higher heating rates. However, this fuel produces a low amount of tars, and it is less affected by the heating rate.

Figure 3 shows the gas produced during the co-gasification of the PT-CH blends at the two heating rates employed. The results for the PT-OS blends were similar to that of the PT-CH blends and will not be discussed here. At 15 °C min<sup>-1</sup>, there is an increase in CO and CO<sub>2</sub> production with respect to the linear additive rule, especially when low percentages of biomass are used. This behaviour may be due to the different reactivity of CH compared to PT. When these samples are gasified at 15 °C min<sup>-1</sup>, both fuels tend to react independently of each other in a different range of temperatures. Thus, the biomass has a higher availability of oxygen at low temperatures, favouring the combustion of volatiles and tars released by the biomass, and so more CO and CO<sub>2</sub> is produced.

Figure 4 shows the carbon loss in tars during the co-gasification of the different blends. As can be seen, there is a clear reduction in carbon loss during the co-gasification of the PT-CH blends at 15 °C min<sup>-1</sup>. However, at 100 °C min<sup>-1</sup> a significant reduction in CO and H<sub>2</sub> production can be observed (Figure 3). This is due to the loss of carbon in tars. As can be seen in Figure 4, the loss of carbon for the PT-PC blends is higher than expected. This leads to a reduction in the amount of sample gasified and in turn the amount of gas produced. As mentioned above, a low availability of oxygen may increase the production of tar. At 100 °C min<sup>-1</sup> the conversion of both, PT and CH, takes place over a shorter interval of time than at 15 °C min<sup>-1</sup>. For this reason, biomass may have the effect of reducing the concentration of

oxygen through the bed, leading to a reduction in the oxidation of volatiles released by PT and to the generation of more tars.

During the gasification of the PT-PC blends at  $15\text{ }^{\circ}\text{C min}^{-1}$ , there is an increase in  $\text{CO}_2$  production and a decrease in  $\text{H}_2$  in comparison with the values predicted by the linear additive rule (Figure 5). These blends present a behaviour similar to that of the PT-CH and PT-OS blends, also due to the different reactivity of the fuels. At low heating rates, PT has more time to react with oxygen, as PC reacts at higher temperatures. For this reason, the oxidation reaction is more pronounced. This has the effect of reducing the carbon consumed through gasification reactions, leading to a decrease in  $\text{H}_2$  production. However at  $100\text{ }^{\circ}\text{C min}^{-1}$ , the PT-PC blends show a different behaviour than the coal and biomass blends and, although the production of  $\text{H}_2$ ,  $\text{CO}$  and  $\text{CO}_2$  is reduced with respect to the theoretical values, it is to a lesser degree. Additionally, the loss of carbon in tar during the gasification of the PT-PC blends at  $100\text{ }^{\circ}\text{C min}^{-1}$  is more linear than in the case of the other blends, with only a slight increase at this heating rate (cf. Figure 4). The differences between these blends may be due to the different volatile matter content of the blended fuels. Biomass releases a high amount of volatiles and modifies the oxidation of the tars produced by coal PT, leading to an increase in tar production. In contrast, PC releases a small amount of volatile matter during the devolatilisation step and the effect on PT is less pronounced.

An important parameter in gasification is the apparent thermal efficiency. This is defined as the ratio of the energy in the gas to the energy in the solid fed in.<sup>19</sup> Figure 6 shows the apparent thermal efficiency obtained during the co-gasification of the PT-CH, PT-OS and PT-PC blends at  $15$  and  $100\text{ }^{\circ}\text{C min}^{-1}$ . The apparent thermal efficiency of the individual fuels increases with the heating rate used during gasification, as more  $\text{CO}$  and  $\text{H}_2$  is produced. At  $15\text{ }^{\circ}\text{C min}^{-1}$ , coal PT and the biomass blends show a slight positive deviation from the additive rule. This could be due to the increase in  $\text{CO}$  production during the co-gasification of these blends. However, the PT-PC blends show a clear reduction in the apparent thermal efficiency, as a consequence of the diminution in  $\text{H}_2$  production. A decrease in the apparent thermal efficiency is observed at  $100\text{ }^{\circ}\text{C min}^{-1}$  for all the blends studied, due to the reduction in  $\text{H}_2$  and  $\text{CO}$  production, especially in the case of the PT-CH blends.

## Conclusions

Co-pyrolysis and co-gasification tests were performed on binary blends of a bituminous coal (PT) with a petcoke (PC) and two types of biomass (CH, OS), using a fixed bed reactor. The results obtained during the co-pyrolysis experiments show that there is no interaction between

the components of the blends. The concentration of the main gases produced during the tests ( $\text{H}_2$ ,  $\text{CO}$ ,  $\text{CO}_2$  and  $\text{CH}_4$ ) was determined, and it was found that they can be calculated from those of the individual fuels and their respective mass fractions. In addition, the mass distribution in char, liquid and gas also follows the linear additive rule.

Gasification tests were performed with mixtures of oxygen, steam and nitrogen at two heating rates, 15 and 100  $^\circ\text{C min}^{-1}$ . At higher heating rates, the individual fuels produce more  $\text{H}_2$  and there is an increase in tar production from the biomass samples due to an increase in the devolatilisation rate and a lower oxygen availability. Different behaviours were observed during the co-gasification results, which were dependant on the heating rate used. At 15  $^\circ\text{C min}^{-1}$ , the components of the blend tend to react independently of each other and there is an increase in  $\text{CO}$  and  $\text{CO}_2$  production due to a higher availability of oxygen for the most reactive components of the blend. For blends of coal and biomass gasified at 100  $^\circ\text{C min}^{-1}$  a decrease in  $\text{H}_2$  and  $\text{CO}$  production was observed due to an increase in carbon loss in tars. However, the behaviour of the PT-PC blend at 100  $^\circ\text{C min}^{-1}$  is different. In this case gas production is almost linear and shows only a slight increase in carbon loss in tars.

## References

1. Midilli A, Ay M, Dincer I, Rosen MA, On hydrogen and hydrogen energy strategies. I: current status and needs. *Renewable and Sustainable Energy Reviews* **9**, pp. 255-271 (2005).
2. European Commission, COM (97)599 final, Energy for the future: Renewable sources of energy ((1997).
3. European Commission, EUR 20719 EN, Hydrogen Energy and Fuel Cells. A vision of our future. Luxembourg: Office for Official Publications of the European Communities, 36 pp., ISBN 92-894-5589-6 (2003).
4. Dunn S, Hydrogen futures: toward a sustainable energy system. *International Journal of Hydrogen Energy* **27**, pp. 235-264 (2002).
5. Song X, Guo Z, Technologies for direct production of flexible  $\text{H}_2/\text{CO}$  synthesis gas. *Energy Conversion and Management*, **47**, pp. 560–569 (2005).
6. González JF, Gañán J, Ramiro A, González-García CM, Encinar JM, Sabio E, Román S, Almond residues gasification plant for generation of electric power. Preliminary study. *Fuel Processing Technology*, **87**, pp. 149-155 (2006).



7. André RN, Pinto F, Franco C, Dias M, Gulyurtlu I, Matos MAA, Cabrita I, Fluidised bed co-gasification of coal and olive oil industry wastes. *Fuel*, **84**, pp. 1635-1644 (2005).
8. Priyadarsan S, Annamalai K, Sweeten JM, Holtzapple MT, Mukhtar S, Co-gasification of blended coal with feedlot and chicken litter biomass. *Proceedings of the Combustion Institute*, **30**, pp. 2973-2980 (2005).
9. Filippis P, Borgianni C, Paolucci M, Pochetti F, Prediction of syngas quality for two-stage gasification of selected waste feedstocks. *Waste Management*, **24**, pp. 633-639 (2004).
10. Ponzio A, Kalisz S, Blasiak W, Effect of operating conditions on tar and gas composition in high temperature air/steam gasification (HTAG) of plastic containing waste. *Fuel Processing Technology*, **87**, pp. 223-233 (2007).
11. Faaij APC. Bio-energy in Europe: changing technology choices. *Energy Policy*, **34**, pp. 322–342 (2006).
12. Albertazzi S, Basile F, Brandin J, Einvall J, Hulteberg C, Fornasari G, Rosetti V, Sanati M, Trifirò F, Vaccari A, The technical feasibility of biomass gasification for hydrogen production. *Catalysis Today*, **106**, pp. 297–300 (2005).
13. Strezov V, Patterson M, Zymła V, Fisher K, Evans TJ, Nelson PF, Fundamental aspects of biomass carbonisation. *Journal of Analytical and Applied Pyrolysis*, **79**, pp. 91-100 (2007).
14. Shafizadeh F, Introduction to pyrolysis of biomass. *Journal of Analytical and Applied Pyrolysis*, **3**, pp. 283-305 (1982).
15. Pan GP, Velo E, Puigjaner L, Pyrolysis of blends of biomass with poor coals. *Fuel*, **75**, pp. 412-418 (1996).
16. Biagini E, Lippi F, Petarca L, Tognotti L, Devolatilization rate of biomasses and coal-biomass blends: an experimental investigation. *Fuel*, **81**, pp. 1041-1050 (2002).
17. Collot AG, Zhuo Y, Dugwell DR, Kandiyoti R, Co-pyrolysis and co-gasification of coal and biomass in bench-scale fixed-bed and fluidised bed reactors. *Fuel*, **78**, pp. 667-679 (1999).
18. Meesri C, Moghtaderi B, Lack of synergetic effects in the pyrolytic characteristics of woody biomass/coal blends under low and high heating rate regimes. *Biomass and Bioenergy*, **23**, pp. 55–66 (2002).

19. Gil J, Aznar MP, Caballero MA, Francés E, Corella J, Biomass gasification in fluidized bed at pilot scale with steam-oxygen mixtures. Product distribution for very different operating conditions. *Energy & Fuels*, **11**, pp. 1109-1118 (1997).

## Figure captions

Fig. 1. H<sub>2</sub> (red symbols), CO (blue symbols) and CO<sub>2</sub> (black symbols) production (mol/kg sample) during the co-pyrolysis tests of the PT-CH, PT-OS and PT-PC blends.

Fig. 2. Char (red symbols) and liquid (black symbols) mass distribution during the co-pyrolysis tests of the PT-CH, PT-OS and PT-PC blends.

Fig. 3. Gas production during the co-gasification tests of the PT-CH blends at 15 °C min<sup>-1</sup> (a), and 100 °C min<sup>-1</sup> (b).

Fig. 4 Carbon loss in tar during the co-gasification of the PT-CH, PT-OS and PT-PC blends at 15 °C min<sup>-1</sup> (a), and 100 °C min<sup>-1</sup> (b).

Fig. 5. Gas production during the co-gasification tests of the PT-PC blends at 15 °C min<sup>-1</sup> (a), and 100 °C min<sup>-1</sup> (b).

Fig. 6. Apparent thermal efficiency during the co-gasification of the PT-CH, PT-OS and PT-PC blends at 15 °C min<sup>-1</sup> (red symbols), and 100 °C min<sup>-1</sup> (black symbols).

Table 1. Proximate and ultimate analyses and high heating values of the samples

Sample	Proximate analysis (wt.%)				Ultimate analysis (wt.%, daf)					HHV (MJ/kg)
	Moisture	Ash (db)	Volatile matter (db)	Fixed carbon* (db)	C	H	N	S	O*	
PT	4.2	39.3	23.8	36.9	74.5	5.1	1.6	1.5	17.3	17.6
PC	0.4	0.4	10.6	89.0	88.1	3.8	1.6	5.7	0.8	34.5
CH	8.5	1.2	80.7	18.1	50.3	5.8	0.1	0.0	43.8	17.6
OS	7.7	0.5	82.4	17.1	50.9	6.0	0.1	0.0	43.0	17.7

\*calculated by difference

db: dry basis

daf: dry and ash free basis

Table 2. Gas production and carbon mass distribution during the pyrolysis tests

Sample	Gas production (mol/kg <sub>sample</sub> )				Carbon mass distribution (%)		
	H <sub>2</sub>	CO	CO <sub>2</sub>	CH <sub>4</sub>	Gas	Char	Liquids
PT	6.8	1.1	0.6	1.2	15.5	61.7	22.8
CH	4.1	2.4	2.0	1.1	24.7	20.0	55.3
OS	5.2	2.0	2.3	1.1	22.4	18.6	59.0
PC	12.9	0.2	0.2	2.1	7.0	89.1	3.9

Table 3. Gas production (mol/kg<sub>sample</sub>) and carbon loss in the tars during the gasification of the individual fuels at 15 and 100 °C min<sup>-1</sup>

Sample	15 °C min <sup>-1</sup>					100 °C min <sup>-1</sup>				
	H <sub>2</sub>	CO	CO <sub>2</sub>	CH <sub>4</sub>	% C <sub>loss</sub>	H <sub>2</sub>	CO	CO <sub>2</sub>	CH <sub>4</sub>	% C <sub>loss</sub>
PT	21.1	13.3	15.3	1.1	21.2	29.3	18.6	14.0	1.7	8.9
CH	8.9	6.4	17.4	0.8	40.6	13.8	12.2	6.8	0.8	52.2
OS	13.2	5.8	16.1	1.0	45.7	14.2	12.1	6.6	0.7	54.0
PC	40.0	21.9	45.1	2.3	5.2	48.2	25.0	47.5	2.6	0.0

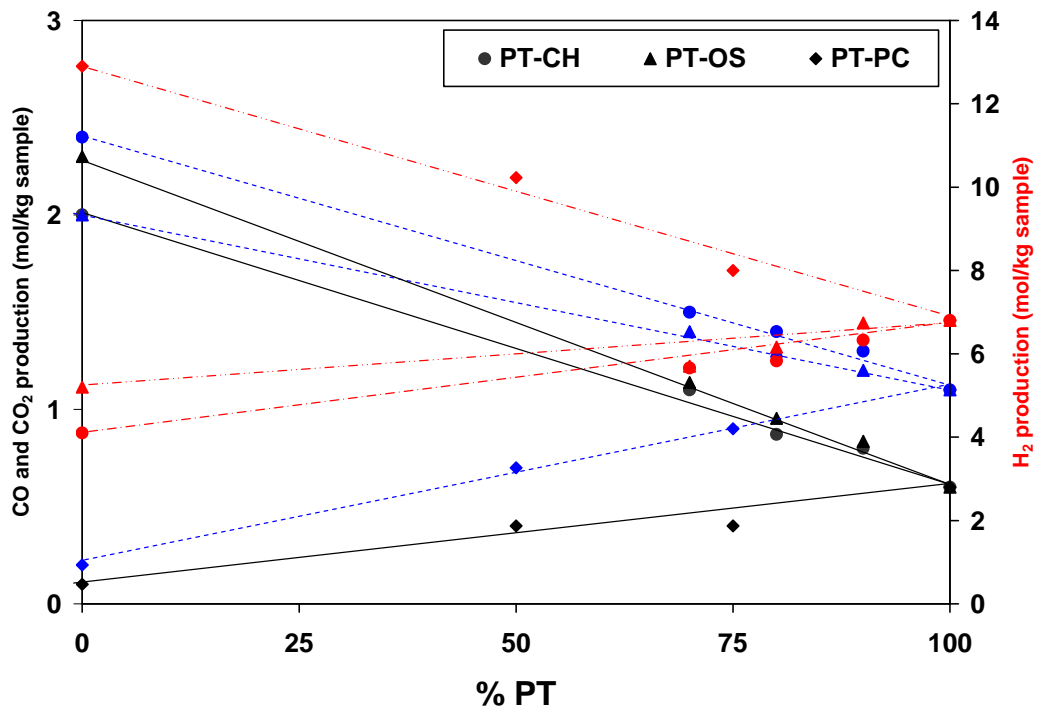


Figure 1. H<sub>2</sub> (red symbols), CO (blue symbols) and CO<sub>2</sub> (black symbols) production (mol/kg sample) during the co-pyrolysis tests of the PT-CH, PT-OS and PT-PC blends.

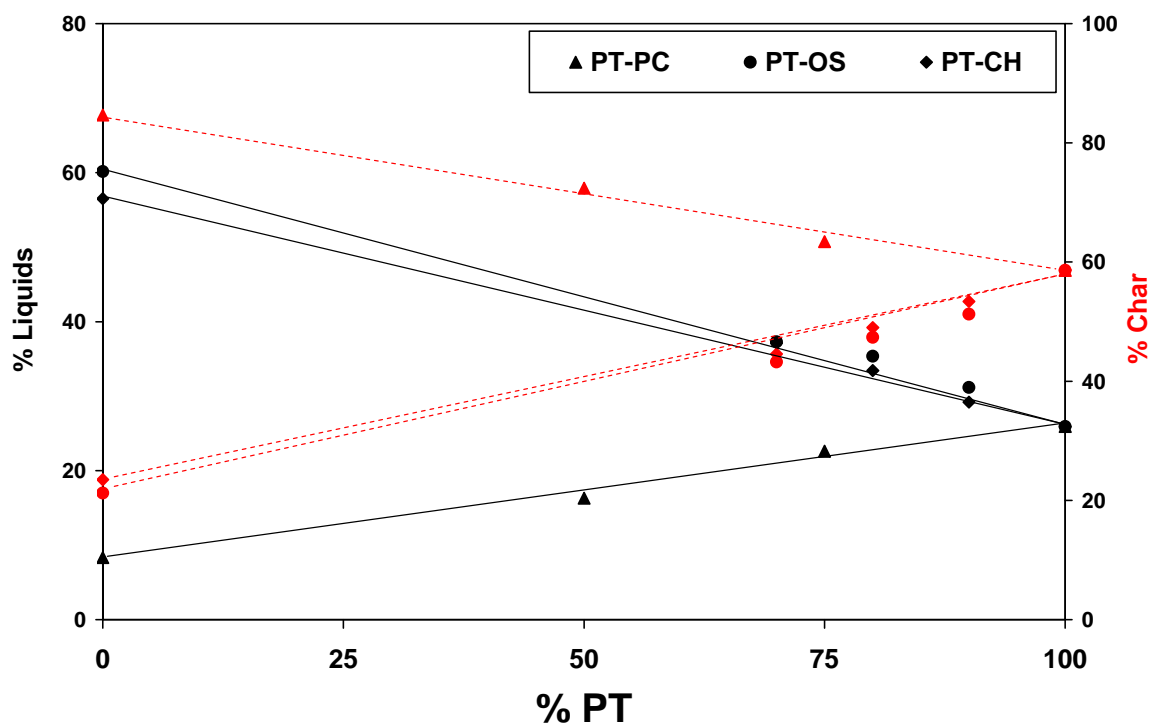


Figure 2. Char (red symbols) and liquid (black symbols) mass distribution during the copyrolysis tests of the PT-CH, PT-OS and PT-PC blends.



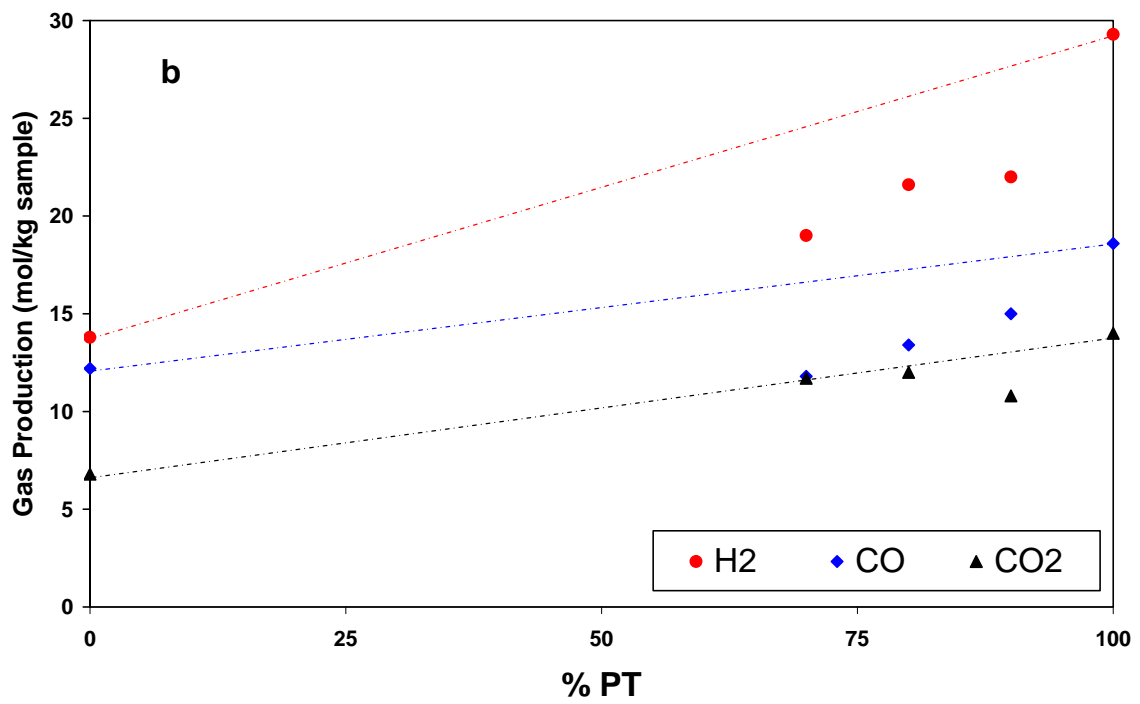
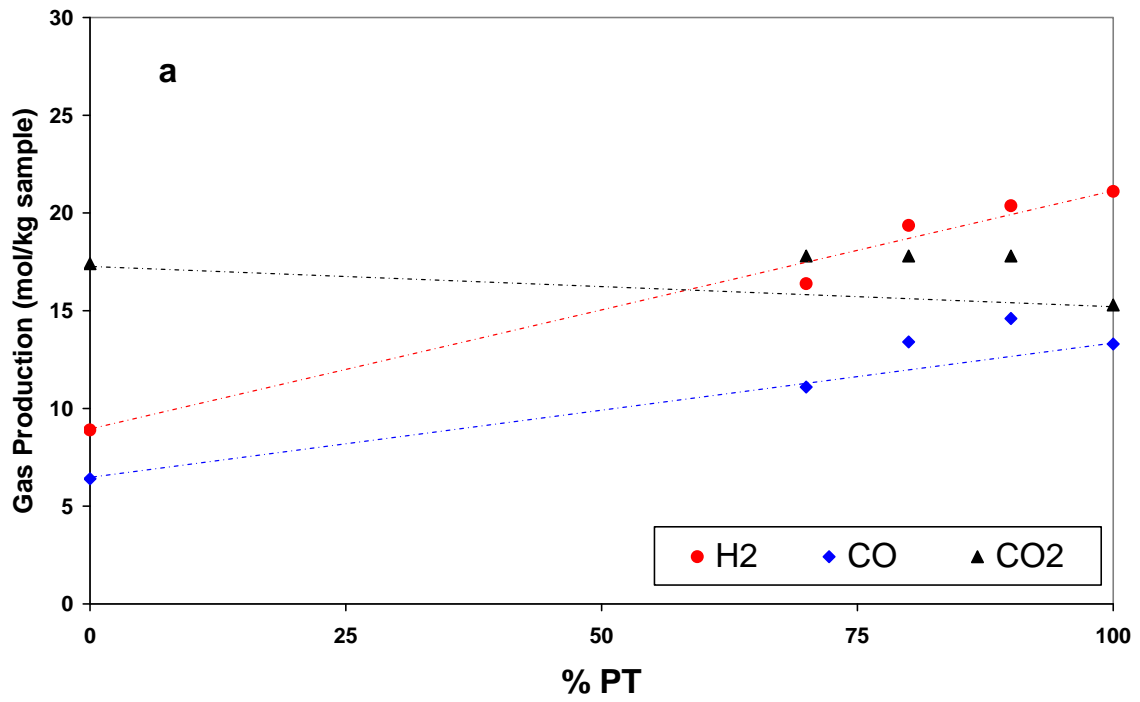


Figure 3. Gas production during the co-gasification tests of the PT-CH blends at 15 °C min<sup>-1</sup> (a), and 100 °C min<sup>-1</sup> (b).

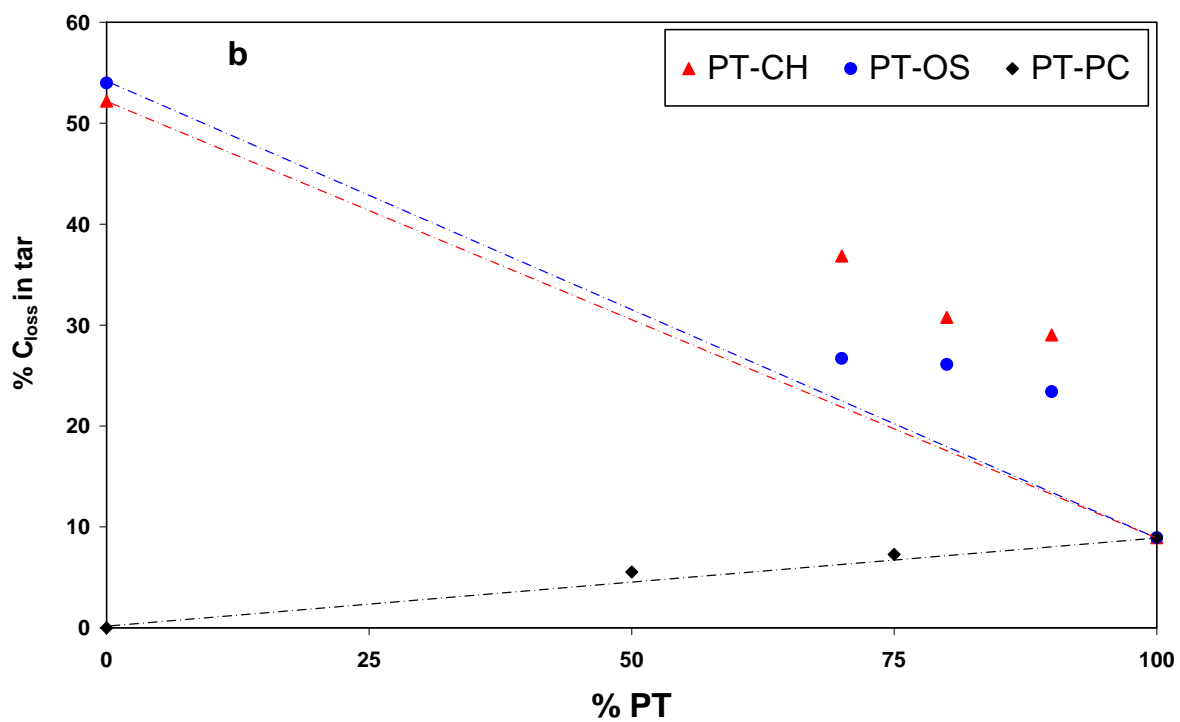
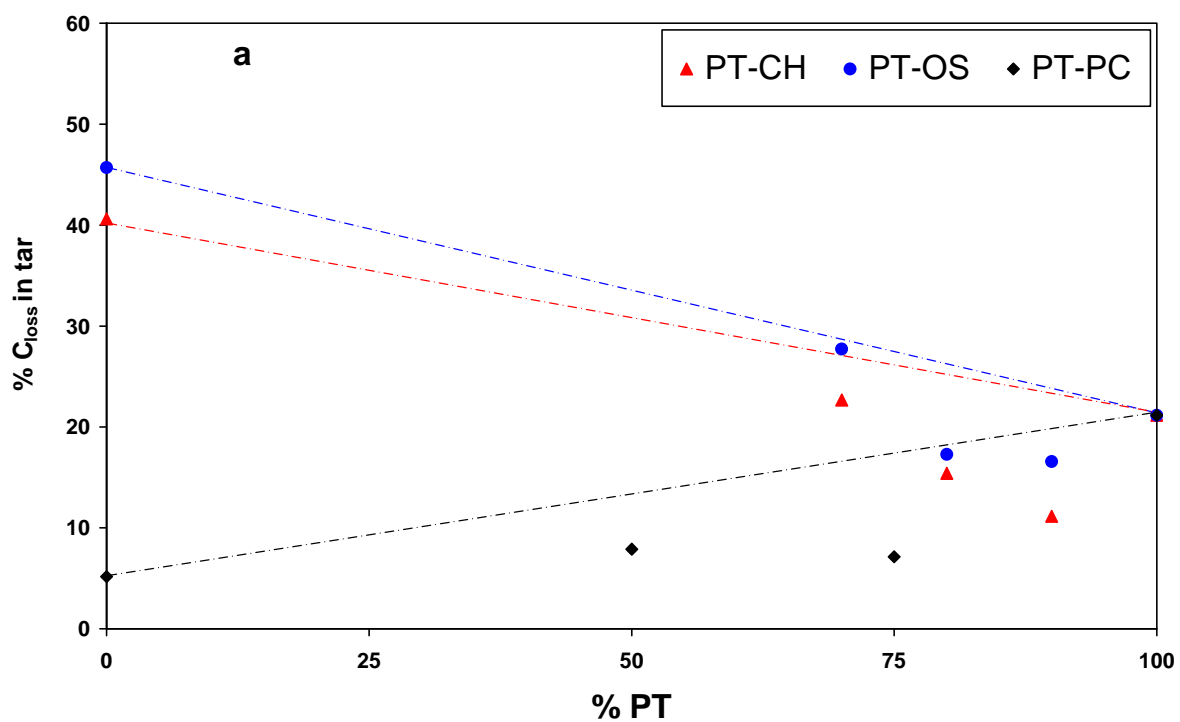


Figure 4. Carbon loss in tar during the co-gasification of the PT-CH, PT-OS and PT-PC blends at 15 °C min<sup>-1</sup> (a), and 100 °C min<sup>-1</sup> (b).

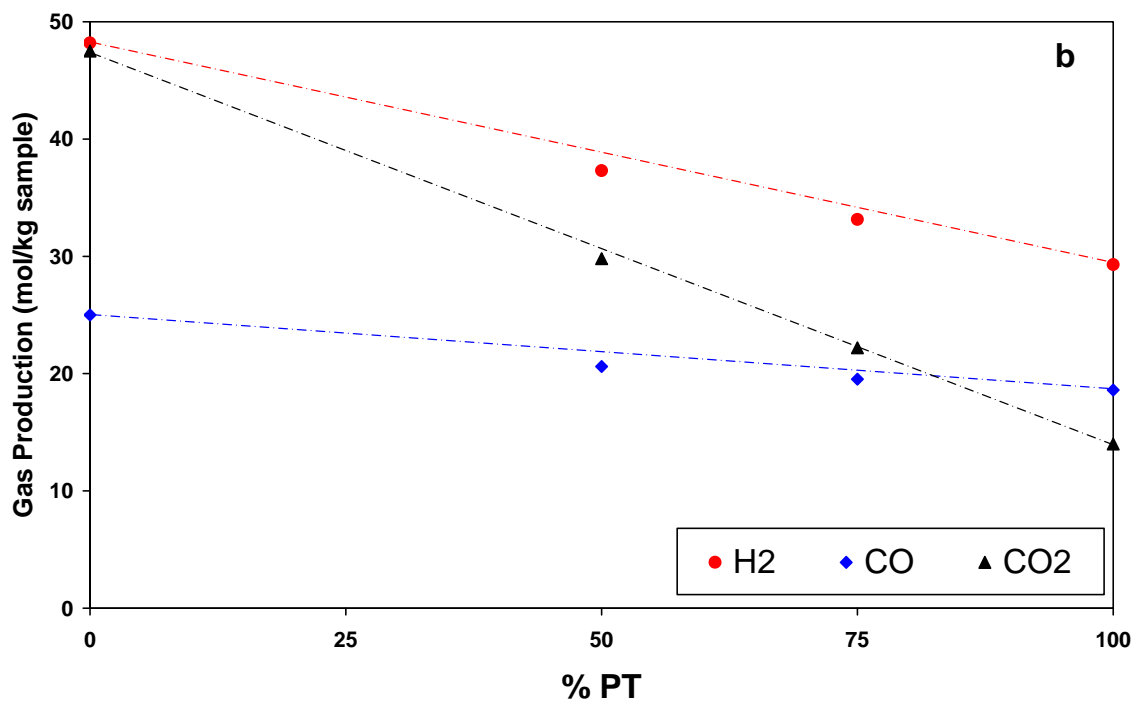
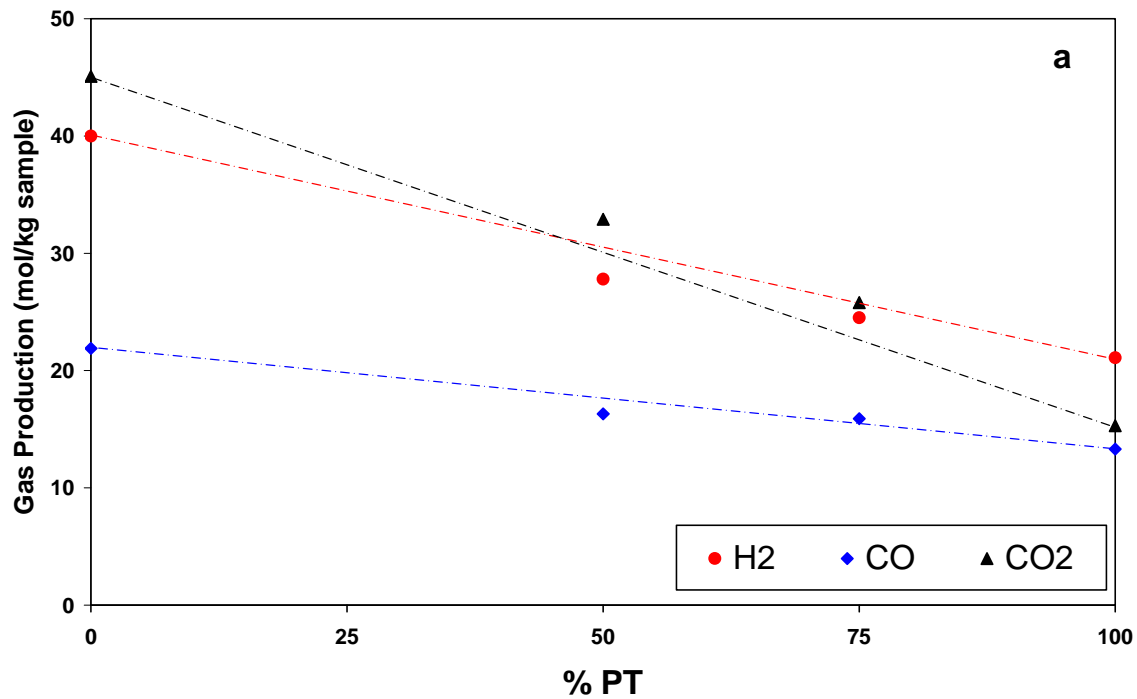


Figure 5. Gas production during the co-gasification tests of the PT-PC blends at 15 °C min<sup>-1</sup> (a), and 100 °C min<sup>-1</sup> (b).

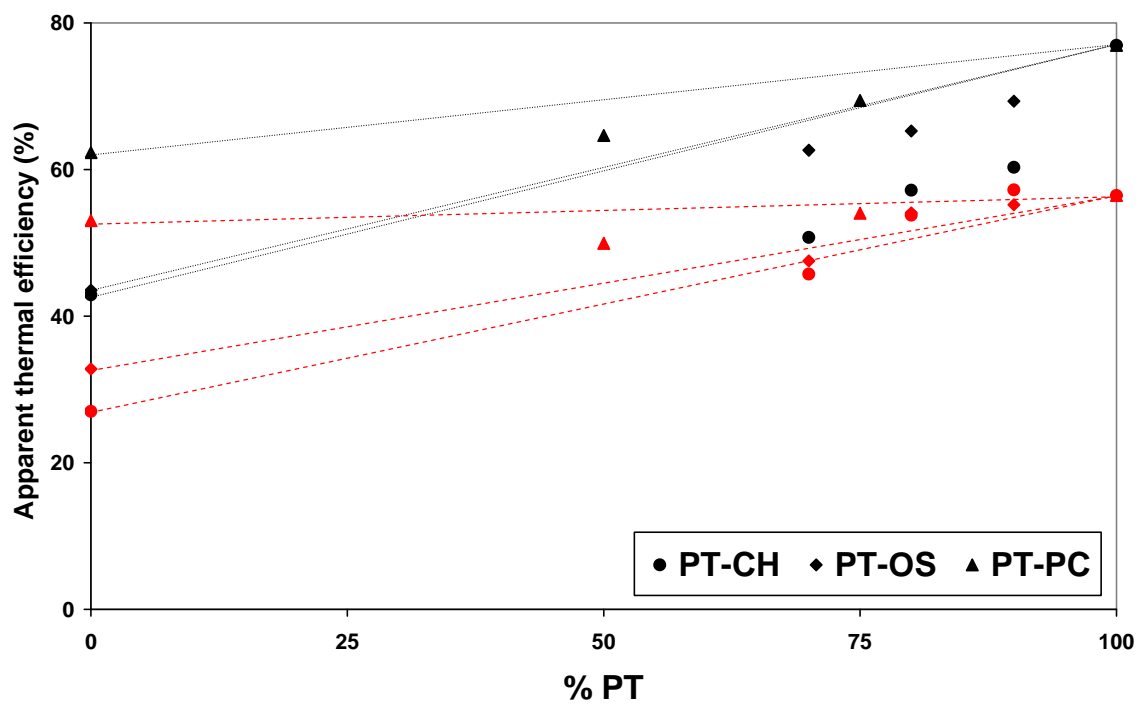


Figure 6. Apparent thermal efficiency during the co-gasification of the PT-CH, PT-OS and PT-PC blends at 15 °C min<sup>-1</sup> (red symbols), and 100 °C min<sup>-1</sup> (black symbols).